Central European Journal of Energetic Materials, **2006**, *3*(3), 15-25.
ISSN 1733-7178

Lithium Manganate Grown from Water-Solubility Explosive with EPS

Xinghua XIE, Hongbo WU, Weiguo WANG, Meng WANG, Wenyao HUANG

Department of Chemical Engineering,
Anhui University of Science and Technology,
Huainan 232001, China
E-mail: xhxie@aust.edu.cn

Xiaojie LI

Department of Engineering Mechanics,
Dalian University of Technology,
Dalian 116024, China

Abstract: Nanostructured spherical spinel lithium manganate with about 30 nm in diameter was synthesized for the first time by explosive method. The water-solubility explosive was prepared using a simple facility at room temperature. The growth of lithium manganate *via* detonation reaction was investigated with respect to the presence of an energetic precursor, such as the metallic nitrate and the degree of confinement of the explosive charge. The detonation products were characterized by scanning electron microscopy. Powder X-ray diffraction and transmission electron microscopy were used to characterize the products. Lithium manganate with spherical morphology and more uniform secondary particles, with smaller primary particles of diameters from 10 to 50 nm and a variety of morphologies were found. Lithium manganate with a fine spherical morphology different from that of the normal spinel is formed after detonation wave treatment due to the very high quenching rate. It might also provide a cheap large-scale synthesis method. Explosive detonation is strongly nonequilibrium processes, generating a short duration of high pressure and high temperature. Free metal atoms are first released with the decomposition of explosives, and then theses metal and oxygen atoms are rearranged, coagulated and finally crystallized into lithium manganate during the expansion of detonation process.

Keywords: nanostructures, lithium compounds, manganites, detonation synthesis, epispastic polystyrene (EPS)

Introduction

The spinel lithium manganate synthesized by the conventional method has several disadvantages, such as inhomogeneity, irregular morphology, large particle size, broad particle size distribution, high synthesis temperature and repeated grinding. To overcome the disadvantages of solid-state reaction, several soft chemistry methods, such as hydrothermal method, sol–gel, solvothermal method, coprecipitation and pechini process have been developed. Among these methods, solvothermal method should use organic agents. It is toxic and unsafe. The sol–gel, coprecipitation and pechini process need further calcinations and grinding. The hydrothermal synthesis is a powerful method to prepare various oxides. The advantage features of this method are to control the morphology, the particle size and the crystalline of products. However, most spinel Li-Mn-O products synthesized by the hydrothermal method reported in literature were powders with irregular shapes.

A. Singhal *et al.* [1] thought that nanostructured intercalating electrodes offer immense potential for significantly enhancing the performance of rechargeable rocking chair.

Shuhua Ma *et al.* [2] said that spinel structure Li-Mn-O compounds are the most promising lithium ion insertion electrode materials for rechargeable lithium ion batteries because of a number of advantages over their alternatives, e.g., a lower cost compared with $LiCoO_2$ or $LiNiO_2$, a high cell voltage, and a high environmental tolerance, etc. The excess of Li and substitution of Cr to Mn and small surface area impeded the occurrence of the split. The split is presumably considered relating to the disproportionation dissolution of stoichiometric spinel intensified by the elevated temperatures in slightly acidic electrolyte due to residual water impurity. Li-Mn-O can selectively insert Li from an aqueous solution [3].

Mitsuharu Tabuchi *et al.* [4] reported that the excess Li could substitute the Mn ion on the 16d site in the spinel structure. And they introduced excellent cycling behavior for nonstoichiometric $Li_{1.0}Mn_{1.93}O_4$. Jong-Uk Kim *et al.* [5] investigated characteristics of charge/discharge cycling of $LiMn_2O_4$. I.J. Davidson *et al.* [6] reported that using solid-state reactions method, however, the powder preparation route is also quite complicated, for example, several times calcinations and subsequent physical grindings. Moreover, its electrochemical properties are greatly dependent on its crystalline particle size [7].

Zhanqiang Liu *et al.* [8] synthesized nanostructured spherical spinel lithium manganese oxide (Li-Mn-O) with about 200 nm in diameter for the first time by mild hydrothermal method, and studied systematically the influence of the reaction temperature and the time of formation of the nanostructures.

Until now, there are a few reports concerning high-capacity maintainable lithium manganate synthesized by detonation of explosives, which is a kind of promising technique for synthesis of lithium transition metal oxide cathodes. Here, for the first time, lithium manganate was synthesized from water-solubility explosive with epispastic's polystyrene (EPS).

Experimental

Water-solubility explosive preparation

The water-solubility explosive was prepared using a simple facility consisting of a container equipped with a stirrer. $LiNO_3$, NH_4NO_3, Mn $(NO_3)_2$ (50 wt.% solution in water) and glycol were mixed in a desired proportions and stirred until a uniform solution was formed. The solution of oxidizers and glycol was agitated at room temperature and then slowly added to a transparent polyester bottle, in which a premixed mixture of epispastic polystyrene (EPS) fine spheres with fine cyclotrimethylene trinitramine (RDX) powders were filled in fully. The water-solubility explosive charges were put into the thin plastic bottle fully with an approximate 660 kg m^{-3} density and the mass was fixed at 0.420 kg of explosive matter. For each charge an electric No. 8 initiator and a 0.008 kg plastic RDX booster were used. The detonation experiments were performed in an explosive chamber (shown in Figure 1).

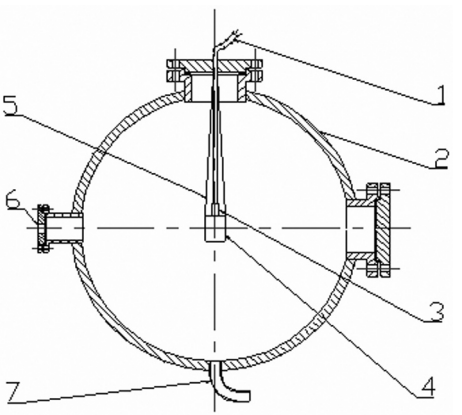

Figure 1. Schematic explosive chamber:
1 – powerline; 2 – explosive chamber; 3 – detonator; 4 – explosive; 5 – lifting rope; 6 – exhausting hole; 7 – deslagging pipe.

This method provides a very fast quenching space. The air surrounding the charge provides efficient cooling of detonation products and thus reduces the reuniting of obtained nanoparticles. The detonation experiments were done in a steel tank of 14.1 m^3. The explosive charge was placed in a polyethylene bag, which was suspended at the tank center. The detonation products contained some impurities such as fragments from the tank walls (Fe_2O_3, Al_2O_3), copper and steel from the detonator, and PE from the bag and the leg wires of the detonator. Large size impurities were eliminated by simple filtration of the suspension. The solid residue was washed thoroughly and dried. All the final products were analyzed by X-ray diffractometry (XRD) [$\lambda_{CuK\alpha}$ = 1.5406 Å] in the range of 10-80° (2θ). So for all the experiments, the detonation of water-solubility explosives synthesized a black powder containing mainly ultradispersed composite oxides of lithium manganate.

Experimental apparatus for samples

After annealing at 400 °C for 6 hours, the detonation soot was studied by use of XRD. Scanning electron microscopy (SEM) analysis was performed with JEOL JEM-1200EX for detonation synthesized lithium manganate. XRD analysis was performed on an XRD-6000 Shimadzu diffractometer using Cu Kα irradiation with input power of 50 kV and 150 mA. The divergence slit angle, scattering slit angle and receiving slit height were selected as 2, 2°, and 0.3 mm. The diffraction intensities were measured every step 0.028° for 1 s in the 2θ range from 10 to 80° at room temperature (293 K). The shape and size of the as-obtained particles were observed by transmission electron microscope (TEM, Tecnai G^2 20 S-twin).

Results and Discussion

Detonation temperature and pressure

The exact mechanism of the formation of such nano-grains in the water-solubility explosive derived so far is poorly understood.

The general explosion reaction equation is achieved.

$$1.10LiNO_3 + 1.10Mn(NO_3)_2{\cdot}10H_2O + 1.19C_2H_4(OH)_2 + 3.38NH_4NO_3 + 0.66C_3H_6O_6N_6 + 0.38C_8H_8 \rightarrow 0.55Li_2O + 0.22MnO_2 + 0.44Mn_2O_3 + 2.84CO_2 + 7.01N_2 + 24.83H_2O + 4.56CO$$

We can figure out the detonation temperature t and pressure P_{CJ} of water-solubility explosives as follows.

A method of estimating P_{CJ} at ρ invokes the thermochemical properties [9].

Their empirical relationships are

$$\phi = NM^{1/2} Q^{1/2}, \quad (1)$$

and

$$P_{CJ} = 1.56 \rho_0^2 \phi \quad (2)$$

where: N is moles of gaseous detonation products per g of water-gel explosive (mol gas/g explosive), M is average molecular weight of detonation product gas (g gas/mol gas), and Q is chemical energy of detonation reaction (cal g^{-1}).

If we consider the water of detonation products in liquid state,

$Q_{P\ [H_2O\ (l)]}$ = 0.55×(-595.8) + 0.22×(-521.5) + 0.44×(-959.0) + 2.84×(-393.7) + 24.83×(-242.0) +4.56×(-110.52)- 1.10×(-482.2) - 1.10×(-3432.6) - 1.19×(-452.3) -3.38×(-340.0) -0.66×(+62.0) –0.38×(+220.2) = -327.7 - 114.7 - 422.0 -1118.1 - 6008.9 -504.0 + 530.4 + 3775.9 + 538.2 + 1149.2 -40.9 -83.7 = -2626.3 (kJ kg^{-1})

$Q_{v\ [H_2O\ (l)]}$ = 2626.3 kJ + (2.84 + 7.01 + 24.83 + 4.56)× 8.314×10^{-3}×298.15 kJ = 2723.6 kJ

$$C_{vi} = a + bt \quad (3)$$

$$Q_v = (a + bt)t \quad (4)$$

$$t = \frac{-a + \sqrt{a^2 + 4bQ_v}}{2b} \quad (5)$$

For double atoms in gas phase,

C_v = 20.10 + 1.88×10^{-3} t

For H_2O,

C_v = 16.72 + 8.99×10^{-3} t

For CO_2,

C_v = 37.62 + 2.42×10^{-3} t

For crystals (from the Dulong-Petit's law),

C_v = 3R = 24.94

C_v = (7.01 + 4.56)×(20.10 + 1.88×10^{-3} t) + (0.55 + 0.22)×(3×24.94) + 0.44×(5×24.94) + 2.84×(37.62 + 2.42×10^{-3} t) + 24.83×(16.72 + 8.99×10^{-3} t) = 232.56 + 21.75×10^{-3} t + 57.61 + 54.87 + 106.84 + 6.87×10^{-3} t + 415.16 + 223.22×10^{-3} t = 867.04 + 251.84×10^{-3} t

t = 2288.6 K

N = (2.84 + 7.01 + 24.83 + 4.56)/1000 = 0.03924 (mol g^{-1})

M = (2.84×44+7.01×28+24.83×18 + 4.56×28)/39.24=22.83 (g mol^{-1})

$Q = Q_v$ [H_2O (l)] /4.18 = 651.6 (cal g^{-1})

$\phi = 0.03924 \times 22.83^{1/2}\ 651.6^{1/2} = 4.787$
$P_{CJ} = 1.56 \times 0.660^2 \times 4.787 = 3.25$ (GPa)

XRD structural characterization of samples

Figure 2 shows an XRD pattern of the dynamically synthesized lithium manganate. We obtained a nanosized texture containing spinel lithium manganate. It is obvious that the Bragg reflection peaks of the dynamically synthesized lithium manganate are broadened, which may result form small grain size and/or presence of microstrain. Here the mean grain size for detonation synthesized lithium manganate refers to the mean size of crystallites of polycrystalline particles. XRD analyses were conducted at a fixed temperature in the present study; a precise determination of the structural parameters need more experiments including both high temperature and low temperature experiments. The pattern represents the peak positions expected for $Li_{1.32}Mn_{1.68}O_4$ (JCPDS file n. 88-0459).

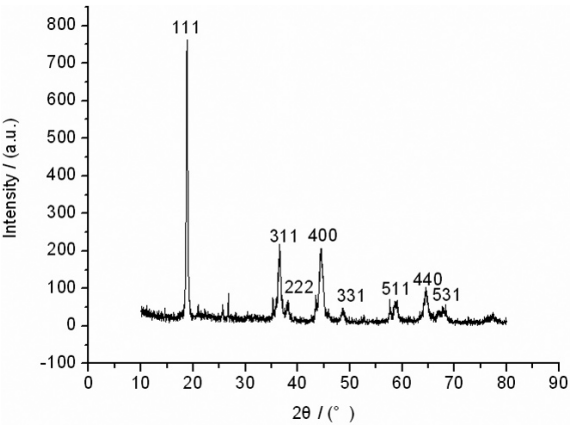

Figure 2. XRD pattern of lithium manganate.

Explosive detonation is strongly nonequilibrium process, generating a short duration of high pressure and high temperature. A most intense $LiMn_2O_4$ line is seen on the x-ray pattern of these products.

V. Berbenni *et al.* [10] reached that $LiMn_2O_4$ forms directly and its formation is completed within 700 °C, and at T > 820 °C $LiMn_2O_4$ reversibly decomposes to $LiMnO_2$ and Mn_3O_4 with an enthalpy of 30.05 kJ mol^{-1} of $LiMn_2O_4$.

The average grain size (D) was measured from the XRD peak using the Scherrer formula [11]:

$$D = 0.9\frac{\lambda}{\beta\cos\theta} \tag{6}$$

where $\lambda = 0.15418$ nm, θ is the Bragg angle of the peak, and β is the full width at half maximum.

The calculated mean grain sizes were 27.10 nm and the crystal constant a = 0.8158 nm for detonation synthesized spinel lithium manganate. P. Piszora *et al.* [12] applied the computer modelling techniques and investigated the Li^+, Mn^{3+} and Mn^{4+} ion distribution by calculating the lattice energy, combined with energy minimisation procedures, using the General Utility Lattice Program (GULP), a program designed for simulation of ionic and semi-ionic solids, based on interatomic potential models. In the series with a nominal $Li_xMn_{3-x}O_4$ stoichiometry, with $0.55 \leq x \leq 2.0$, the well-crystallized cubic spinel phase was accompanied by the tetragonal hausmannite, Mn_3O_4, and/or bixbyite, α-Mn_2O_3, when $x < 1$, whereas the monoclinic Li_2MnO_3 phase was formed beside the spinel phase, for $x > 1.33$ [12].

C. M. Julien *et al.* [13] concluded that spinel structure λ-$LiMn_2O_4$ is primarily characterised by structural groups as follows. (1) MnO_6 octahedra connected to one another in three dimensions by edge sharing; (2) LiO_4 tetrahedra sharing each of their four corners with a different MnO_6 unit but essentially isolated from one another; (3) a three-dimensional network of octahedral 16*c* and tetrahedral (primarily 8*a*) sites, through which lithium ions can move through the lattice. Lithium-/manganese-oxide spinels are, currently, of technologic interest as insertion electrodes for rechargeable 4-V lithium batteries.

SEM and TEM characterization of samples

Scanning electron microscopy and transmission electron microscopy were used to characterize the products. Figures 3 and 4 are morphologies taken by SEM and TEM respectively. Lithium manganate with 30 nm spherical morphology and more uniform secondary particles, with smaller primary particles of diameters from 10 to 50 nm and a variety of morphologies were found.

The SEM micrograph showed agglomeration of primary particles with varied agglomerate size. Although TEM picture shows smaller particles, which are aggregated further to form agglomeration, varied sizes, it is necessary to obtain the information regarding smallest primary particles. For this purpose, the TEM study and selected area electron diffraction (SAED) were shown in Figure 4. The SAED pattern of zinc oxide nanometer powders shows a clear diffraction ring and varied points corresponding to the crystal planes of phase.

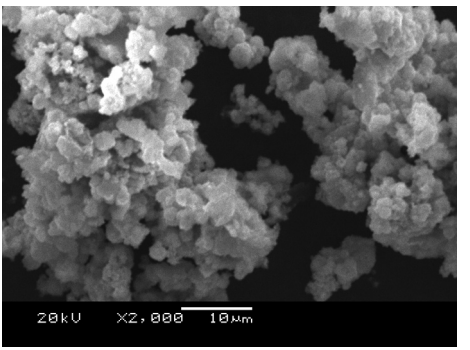

Figure 3. SEM image of detonation synthesized lithium manganate.

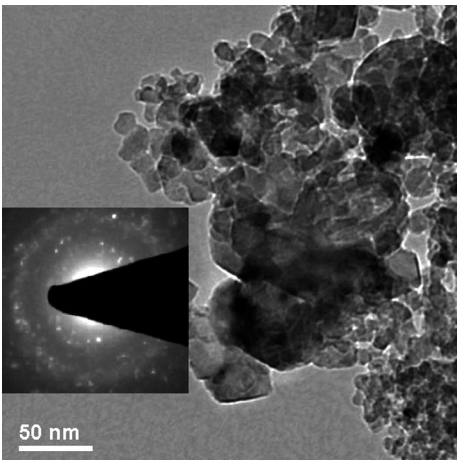

Figure 4. TEM image of detonation synthesized lithium manganate.

Troyanov *et al.* [14] reported that for a mixture of 20% gibbsite and 80% hexogen the theoretical temperature of the explosion is about 2000 °C. Hexogen $C_3H_6N_6O_6$ decomposes into CO_2, CO, H_2O, H and N under explosion. The positive oxygen balance governs the sufficient supply of oxygen in the final effluxes of the explosion.

Moon-Kyu Kim *et al.* [15] concluded that Li-Mn-O synthesized by the emulsion drying shows most capacity loss in the high-voltage region and no capacity loss in the voltage-drop region in the 4 V range; And no capacity loss in the voltage-drop region of the 4 V range indicates that the phase transformation induced by John–Teller distortion is not the cause of capacity loss in the 4 V range.

Yang-Soo Kim *et al.* [16] studied the electronic structure and chemical bonding of the $LiM_{0.5}Mn_{1.5}O_4$ with the use of the DV-Xα molecular orbital method.

All the elements of Hamiltonian and overlap matrices were calculated numerically on the basis of the discrete variational integration scheme. Jun Sugiyama *et al.* [17] discussed the mechanism for formation of oxygen defects using a defect cluster model. $LiMn_2O_{4-\delta}$. The $LiMn_2O_{4-\delta}$ samples with $3.33 < 4-\delta \leq 3.75$ were a mixture of $LiMn_2O_{4-\delta}$, $LiMnO_2$ and Mn_3O_4. Therefore, the maximum oxygen deficiency was found to be $\delta_{cr} = 0.2$.

Yongyao Xia *et al.* [18] suggested that a single spine1 phase exists in the range of $1.0 < x < 1.14$ in $Li_xMn_2O_4$. Vincenzo Massarotti *et al.* [19] concluded that fast cooling inhibited the equilibrium with O_2. This cubic phase is stable at high temperature and decomposes upon cooling ($T \leq 800$ °C) leaving just the Mn_3O_4 and *o*-$LiMnO_2$ phases [20]. Ramesh Chitrakar *et al.* [21] obtained cubic $Li_{1.6}Mn_{1.6}O_4$ by heating *o*-$LiMnO_2$ at 400 °C; lithium could be extracted from $Li_{1.6}Mn_{1.6}O_4$ with acid to form cubic $H_{1.6}Mn_{1.6}O_4$ for possible applications in extraction of lithium from seawater. The simple and efficient approach employed for the nano-lithium and manganese oxide products can be successfully used for the fabrication of $LiMn_2O_4$. Indeed, the advantage of the ability to induce surface modification of $LiMn_2O_4$ makes the method useful as well as usual high-technological methods. Further investigations of different cases may lead to new opportunity for the fabrication of $LiMn_2O_4$ powders with improved properties based on the simple method of detonation synthesis. Y. Shin *et al.* [22] reached that samples with larger and more uniform secondary particles, but with smaller primary particles, are found to give better cyclability despite a higher amount of manganese dissolution arising from smaller primary particles.

Conclusions

Lithium manganate with a fine spherical morphology different from that of the normal spinel is formed after detonation wave treatment due to the very high quenching rate. It might also provide a cheap large-scale synthesis method. Explosive detonation is strongly nonequilibrium processes, generating a short duration of high pressure and high temperature. Free metal atoms are first released with the decomposition of explosives, and then theses metal and oxygen atoms are rearranged, coagulated and finally crystallized into lithium manganate during the expansion of detonation process. The inherent short duration, high heating rate (10^{10}-10^{11} K s^{-1}) and high cooling rate (10^8-10^9 K s^{-1}) prevent the lithium manganate crystallites from growing into larger sizes and induce considerable lattice distortion.

Acknowledgements

Research described in this paper was done possible in part by the grant 10572034 from the Chinese National Natural Science Foundation and from the Anhui Provincial Educational Office.

References

[1] Singhal A., Skandan G., Amatucci G., Badway F., Ye N., Manthiram A., Ye H., Xu J. J., Nanostructured Electrodes for Next Generation Rechargeable Electrochemical Devices, *J. Power Sources,* **2004**, *129*(1), 38-44.

[2] Ma S. H., Noguchi H., Yoshio M., An Observation of Peak Split in High Temperature CV Studies on Li-stoichiometric Spinel $LiMn_2O_4$ Electrode, *ibid.,* **2004**, *125*(2), 228-235.

[3] Morcrette M., Barboux P., Perrie`re J., Brousse T., $LiMn_2O_4$ Thin Films for Lithium Ion Sensors, *Solid St. Ionics,* **1998**, *112*(3-4), 249-254.

[4] Tabuchi M., Masquelier C., Kobayashi H., Kanno R., Kobayashi Y., Akai T., Maki Y., Kageyama H., Nakamura O., Characterization of $Li_{1-\delta}Mn_{2-2\delta}O_4$ Defect Spinel Materials by Their Phase Transition, Magnetic and Electrochemical Properties, *J. Power Sources,* **1997**, *68*(2), 623-628.

[5] Kim J. U., Jeong I. S., Moon S. I., Gu H. B., Electrochemical Characteristics of $LiMn_2O_4$-polypyrrole Composite Cathode for Lithium Polymer Batteries, *ibid.,* **2001**, *97-98,* 450-453.

[6] Davidson I. J., McMillan R. S., Slegr H., Luan B., Kargina I., Murray J. J., Swainson I. P., Electrochemistry and Structure of $Li_{2-x}Cr_yMn_{2-y}O_4$ Phases, *ibid.,* **1999**, *81–82,* 406-411.

[7] Komaba S., Myung S. T., Kumagai N., Kanouchi T., Oikawa K., Kamiyama T., Hydrothermal Synthesis of High Crystalline Orthorhombic $LiMnO_2$ as A Cathode Material for Li-ion Batteries,, *Solid St. Ionics,* **2002**, *152-153,* 311-318.

[8] Liu Z. Q., Wang W. L., Liu X. M., Wu M. C., Li D., Zeng Z., Hydrothermal Synthesis of Nanostructured Spinel Lithium Manganese Oxide, *J. Solid St. Chem.,* **2004**, *177*(4-5), 1585-1591.

[9] Zukas J. A., Walters W. P., *Explosive Effects and Applications,* Springer-Verlag New York, **1998**, p. 124.

[10] Berbenni V., Marini A., Solid State Synthesis of Lithiated Manganese Oxides from Mechanically Activated Li_2CO_3-Mn_3O_4 Mixtures, *J. Analyt. Appl. Pyrolysis,* **2003**, *70*(2) 437-456.

[11] Lin X. M., Li L. P., Li G. S., Su W. H., Transport Property and Raman Spectra of Nanocrystalline Solid Solutions $Ce_{0.8}Nd_{0.2}O_{2-\delta}$ with Different Particle Size, *Mater. Chem. Phys.,* **2001**, *69*(1-3), 236-240.

[12] Piszora P., Catlow C. R. A., Woodley S. M., Wolska E., Relationship of Crystal Structure to Interionic Interactions in the Lithium-manganese Spinel Oxides, *Comp.*

Chem., **2000**, *24*(5) 609-613.
[13] Julien C. M., Massot M., Lattice Vibrations of Materials for Lithium Rechargeable Batteries III. Lithium Manganese Oxides, *Mater. Sc. Eng. B,* **2003**, *100*(1), 69-78.
[14] Troyanov S. I., Tsvigunov A. N., Khotin V. G., Puzyreva T. B., Detonation Synthesis and Crystal Structure of Six-Layer Silicon Carbide, *Glass and Ceramics,* **2000**, *57*(7-8), 241-242.
[15] Kim M. K., Chung H. T., Um W. S., Park Y. J., Kim J. G., Kim H. G., A Study on the Capacity Loss with Cycling in $Li/Li_xMn_2O_4$ Cell, *Materials Letters,* **1999**, *39*(3), 133-137.
[16] Kim Y. S., No K. S., Chung K. S., Lee J. C., Ooi K., Li^+ Extraction Reactions with Spinel-type $LiM_{0.5}Mn_{1.5}O_4$ (M=Ti, Fe) and Their Electronic Structures, *ibid.,* **2003**, *57*(26-27), 4140-4146.
[17] Sugiyama J., Atsumi T., Hioki T., Noda S., Kamegashira N., Nonstoichiometry and Defect Structure of Spinel $LiMn_2O_{4-\delta}$, *J. Power Sources,* **1997**, *68*(2) 641-645.
[18] Xia Y. Y., Takeshige H., Noguchi H., Yoshio M., Studies on an Li---Mn---O Spinel System (obtained by melt-impregnation) as a Cathode for 4 V Lithium Batteries Part 1. Synthesis and Electrochemical Behaviour of $Li_xMn_2O_4$, *ibid.,* **1995**, *56*(1), 61-67.
[19] Massarotti V., Capsoni D., Bini M., Stability of $LiMn_2O_4$ and New High Temperature Phases in Air, O_2 and N_2, *Solid St. Commun.,* **2002**, *122*(6), 317-322.
[20] Cao J. M., Ji. H. M., Liu J. S., Zheng M. B., Chang X., Ma X. J., Zhang A. M., Xu Q. H., Controllable Syntheses of Hexagonal and Lamellar Mesostructured Lanthanum Oxide, *Materials Letters,* **2005**, *59*(4), 408-411.
[21] Chitrakar R., Kanoh H., Miyai Y., Ooi K., Synthesis of *o*-$LiMnO_2$ by Microwave Irradiation and Study Its Heat Treatment and Lithium Exchange, *J. Solid St. Chem.,* **2002**, *163*(1), 1-4.
[22] Shin Y. J., *Capacity fading mechanisms and origin of the capacity above 4.5 V of spinel lithium manganese oxides,* The University of Texas at Austin, Doctoral Dissertation **2003**.